Reconstruction of Dynamical Systems from Interspike Intervals

Tim Sauer
Department of Mathematical Sciences, George Mason University, Fairfax, Virginia 22030
(Received 15 February 1994)

Attractor reconstruction from interspike interval (ISI) data is described, in rough analogy with Takens' theorem for attractor reconstruction from time series. Assuming a generic integrate-and-fire model coupling the dynamical system to the spike train, there is a one-to-one correspondence between the system states and interspike interval vectors of sufficiently large dimension. The correspondence has an important implication: interspike intervals can be forecast from past history. We show that deterministically driven ISI series can be distinguished from stochastically driven ISI series on the basis of prediction error.

PACS numbers: 05.45.+b

It is a widely known fact that states of finite-dimensional dynamical systems correspond in a one-to-one manner with delay-coordinate vectors, which are vectors of time series measurements of a generic system observable. In the case of low-dimensional chaotic systems, which follow simple evolution laws but produce irregular dynamics, this is a fact of great importance. System analysis of this type is suggested in [1] and an embedding theorem due to Takens [2] (later extended in [3]) established its validity.

The fact that the current system state can be identified using a vector of time series measurements leads to a number of applications, owing to the fact that analysis of the topology and sometimes the geometry of the chaotic attractor underlying the time series can be performed in the proxy state space consisting of the delay-coordinate vectors. Applications include noise filtering [4] and prediction [5,6] of chaotic time series, and control of unstable periodic orbits solely from a time series record [7].

For some time-varying systems, amplitude measurements of an appropriate observable are not possible or desirable, but a series of pulses, or spikes, emitted at regular or irregular time intervals, can be observed. For example, it may be difficult to measure the time trace of the interior electrostatic potentials of a biological cell, but feasible to record its firing times. In other cases, the firing times may carry more information than the amplitudes. A process in which the dynamical information is carried by a series of event timings is called a *point process.* It is common for point processes to exhibit complex aperiodic behavior, and as a result statistical modeling of point processes is a highly developed subject [8]. The main question of this paper is the following: If a point process is the manifestation of an underlying deterministic system, can the states of the deterministic system be identified from the information provided by the point process? This question has been considered previously in [9,10].

In particular, neurobiological systems are often marked by measurable pulses corresponding to a cell reaching a threshold potential, which triggers rapid depolarization, followed by repolarization, which restarts the cycle. The times of these discrete pulses can be recorded. These types of data differ from a time series of an observable measured at regular time intervals. Many hypotheses and models for the description of the time variability of these pulses have been proposed [11].

For concreteness, we make a simple hypothesis connecting an underlying continuous dynamical system to the point process. The time series from the dynamical system is integrated with respect to time; when it reaches a preset threshold, a spike is generated, after which the integration is restarted. This integrate-and-fire model is chosen for its simplicity and potential wide applicability. Cell depolarization models for pulses may operate in this general manner. Neural cells in particular have multiple inputs, and *a priori* are part of a multidimensional dynamical system. However, in the presence of self-organizing or synchronizing influences, the input may effectively have fewer degrees of freedom, although appearing irregular in time. Therefore in our simulations we hypothesize that the input to be integrated is a low-dimensional chaotic attractor. We use the Lorenz attractor and the Rössler attractor as simple representative examples.

Our goal is to develop a model which is as generic as possible, in order to focus on the linkage between continuous dynamics and the interspike intervals (ISI's) produced by them. In particular, we are not trying to model the detailed mechanism of any single system.

Let $S(t)$ denote the signal produced by a time-varying observable of a finite-dimensional dynamical system. Assume that the trajectories of the dynamical system are asymptotic to a compact attractor X. Let Θ be a positive number which represents the firing threshold. After fixing a starting time T_0, a series of "firing times" $T_1 < T_2 < T_3 < \cdots$ can be recursively defined by the equation

$$\int_{T_i}^{T_{i+1}} S(t)\, dt = \Theta. \tag{1}$$

From the firing times T_i, the interspike intervals can be

defined as $t_i = T_i - T_{i-1}$. Figure 1 shows a time trace of the x coordinate of the Lorenz attractor [12], governed by the equations $\dot{x} = \sigma(y-x)$, $\dot{y} = \rho x - y - xz$, $\dot{z} = -\beta z + xy$, where the parameters are set at the standard values $\sigma = 10$, $\rho = 28$, $\beta = 8/3$. The signal $S(t) = [x(t)+2]^2$ is used with threshold $\Theta = 60$ in Eq. (1) to generate the spike train shown.

Note that the mean of the signal $S(t)$ must be positive to create interspike intervals. We use a variety of choices for $S(t)$ in this study. It turns out that if the interspike intervals are finite, and under certain genericity conditions on the underlying dynamics, signal and threshold, the series $\{t_i\}$ of ISI's can be used to reconstruct the attractor X. In other words, there is a one-to-one correspondence between m-tuples of ISI's and attractor states, which associates each vector $(t_i, t_{i-1}, \ldots, t_{i-m+1})$ of ISI's with the corresponding point $x(T_i)$ on the attractor. In analogy with the original Takens's theorem [2] and its generalization [3], the condition $m > 2D_0$ is sufficient, where D_0 is the box-counting dimension of the attractor X. (See [13] for a precise statement of the theorem hypotheses and proof.) As with Takens's theorem, smaller m may be sufficient in particular cases.

Figure 2 shows a phase portrait reconstructed from interspike intervals. The Rössler equations [14] are $\dot{x} = -(y+z)$, $\dot{y} = x + ay$, $\dot{z} = bx - cz + xz$, where the parameters are set at the standard values $a = 0.36$, $b = 0.4$, $c = 4.5$. Interspike intervals are produced as in (1), where $S(t) = x(t) + 40$ and $\Theta = 20$. The time intervals t_i are recorded, and 150 of the vectors (t_i, t_{i-1}, t_{i-2}) are plotted in Fig. 2(a), connected by straight lines. Figure 2(b) is a plot of 10 000 ISI vectors produced by Eq. (1).

One practical consequence of such a theorem is that the ISI vectors $(t_i, \ldots, t_{i-m+1})$ can be used to reconstruct the attractor X sufficiently to make measurements of dynamical invariants of X possible, and to do short-term prediction on the series $\{t_i\}$. Thus the possibility exists of predicting future interspike intervals from past history, which has practical applications. To explain the meaning of short term, it is instructive to recall the time series case. For chaotic time series, the length of time horizon for which prediction is effective depends on the separation time of nearby trajectories, and so inversely on the largest Lyapunov exponent. For ISI series, the horizon depends both on the Lyapunov exponents of the underlying process and on the threshold Θ. As Θ increases, the predictability decreases.

We will apply a simple version of a nearest-neighbor prediction algorithm (see, for example, [15]). More sophisticated nonlinear prediction algorithms exist; see [6] for examples. The simple version used here is sufficient to diagnose determinism in the series and makes our main results easy to reproduce. In order to quantify the predictability of the series of ISI's we will use the concept of surrogate data [16] to produce statistical controls.

The prediction algorithm works as follows. Given an ISI vector $V_0 = (t_{i_0}, \ldots, t_{i_0-m+1})$, the 1% of other reconstructed vectors V_k that are nearest to V_0 are collected. (It is important to omit vectors V_k which are close to V_0 in time; otherwise prediction degenerates to an in-sample interpolation fit.) The values of the ISI for some number h of steps into the future are averaged for all k to make a prediction. That is, the average $p_{i_0} = \langle t_{i_k+h} \rangle_k$ is used to approximate the future interval t_{i_0+h}. The difference $p - t_{i_0+h}$ is the h-step prediction error at step i_0. We could instead use the series mean m to predict at each step; this h-step prediction error is $m - t_{i_0+h}$. The ratio of the root mean square errors of the two possibilities (the nonlinear prediction algorithm and the constant prediction of the mean) gives the normalized prediction error

$$\mathrm{NPE} = \frac{\langle (p_{i_0} - t_{i_0+h})^2 \rangle^{1/2}}{\langle (m - t_{i_0+h})^2 \rangle^{1/2}}, \tag{2}$$

where the averages are taken over the entire series. The normalized prediction error is a measure of the (out-of-sample) predictibility of the ISI series. A value of NPE less than 1 means that there is linear or nonlinear predictability in the series beyond the baseline prediction of the series mean.

Our goal in predicting ISI's is to verify that the nonlinear deterministic structure of the dynamics that produced the intervals is preserved in the ISI's. Linear au-

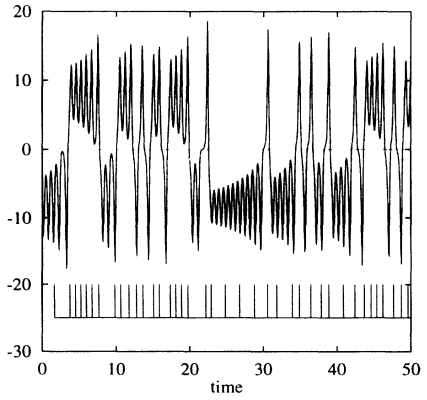

FIG. 1. The upper trace $x(t)$ is the x coordinate of the Lorenz attractor graphed as a function of time. The lower trace shows the times at which spikes are generated according to Eq. (1), with $S(t) = [x(t)+2]^2$ and $\Theta = 60$.

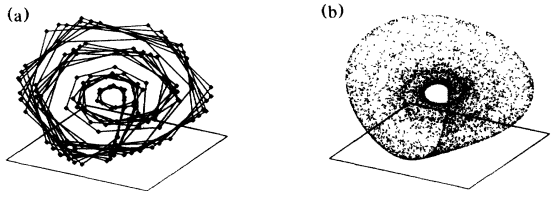

FIG. 2. Reconstructed phase portrait for the Rössler attractor using ISI's. (a) 150 ISI's connected by line segments. (b) 10 000 ISI's shown.

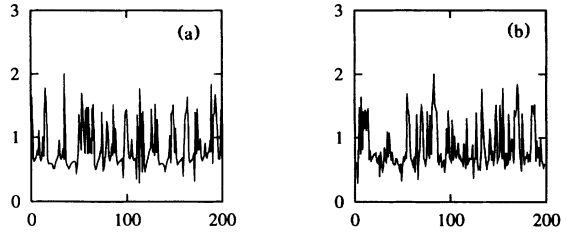

FIG. 3. (a) An ISI series generated by the Lorenz equations, with same parameters as in Fig. 1. (b) A GS surrogate.

tocorrelation in the time series, present for example in correlated noise, can cause NPE to be less than 1. In order to control for this effect, we calculate the NPE for the original series of ISI's as well as for stochastic series of the same length, called surrogate data, which share the same linear autocorrelation and other properties with the original series.

We use two types of surrogate data in our analysis. The first, called a random phase (RP) surrogate, is a series with the same power spectrum as the original series, but is the realization of a stochastic process. (See [16] for further details.) The autocorrelation of the original series is preserved in the new surrogate series, while the nonlinear deterministic structure is eliminated. If the predictability of the original can be shown to be statistically different from the predictability of such surrogates, the null hypothesis that the original series was produced by a Gaussian random process can be rejected, which is evidence that the nonlinear structure of the underlying dynamical system is present in the interspike intervals. The second type of surrogate, called a Gaussian-scaled shuffle (GS) surrogate [16], is a random shuffle of the original series subject to retaining much of the serial correlation. The GS surrogate corresponds to the null hypothesis that the series is a monotonically scaled version of amplitudes produced by a Gaussian random process. Figure 3 shows a section of an ISI series together with a section of a GS surrogate.

The result of applying the nonlinear prediction algorithm to interspike intervals from the Lorenz attractor with $S(t) = [x(t) + 2]^2$ is shown in Fig. 4. For these calculations we fixed the embedding dimension $m = 3$, and predicted one step ahead ($h = 1$). One dozen ISI series, each of length 1024, were generated with varying threshold Θ. For each of the 12 series, two surrogate series of each of the two types were generated. The NPE was computed for each of the 48 series and plotted in Fig. 4. In each of the 12 cases there is a statistically significant difference between the original series and its surrogates. The conclusion is that there is predictability in the ISI series caused by the underlying deterministic dynamics. (More precisely, there is predictability not explained by any of the null hypotheses controlled for by the surrogate data.) As the threshold Θ increases, predictability of the series decreases, and completely disappears near

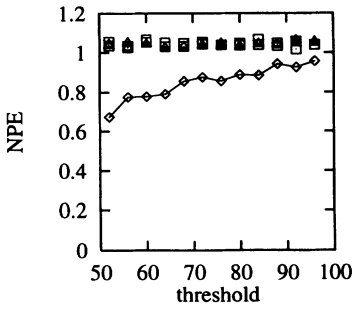

FIG. 4. Normalized one-step ahead prediction error for several ISI series created using the Lorenz attractor, $S(t) = (x + 2)^2$, and thresholds Θ varying on the horizontal axis. Diamonds connected by line segments denote the NPE of the 12 original ISI series; NPE of the surrogates denoted by square (RP) and triangle (GS).

$\Theta = 100$.

In Fig. 5(a), the effect of lengthening the prediction horizon is investigated. A different driving signal is used, $S(t) = (x+y+z)^2$, where x, y, z are the coordinates of the Lorenz equations. The threshold $\Theta = 200$ is fixed. The resulting ISI series has nontrivial linear autocorrelation, which has the effect that NPE < 1 for the surrogates at short prediction horizons. Figure 5(a) shows that there is several-step-ahead predictability in the original ISI series.

A number of tests for deterministic dynamics which can be applied to time series data have been proposed recently [17,18], in addition to calculation of correlation dimension [19]. Nonlinear prediction error is another, relatively powerful distinguishing statistic for this purpose. Now we ask the parallel question for ISI data: Can the deterministic origin of an ISI series be ascertained from the series alone? The following numerical experiment was carried out. Two series of ISI's were generated by Eq. (1). The first is deterministically driven, meaning that $S(t)$ is a signal from the deterministic system used to make Fig. 5(a). The second is stochastically driven: Specifically, $S(t)$ is a realization of a stochastic process which has power spectrum identical to that of the deterministic signal. Figure 5(b) shows the results of the pre-

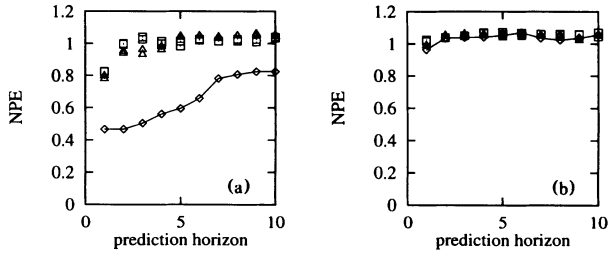

FIG. 5. (a) Diamonds denote NPE as a function of prediction horizon for ISI's created by the Lorenz attractor with $S(t) = (x + y + z)^2$, $\Theta = 200$. NPE of surrogates denoted as in Fig. 4. (b) Same as (a), but with the signal $x + y + z$ replaced by noise with identical power spectrum.

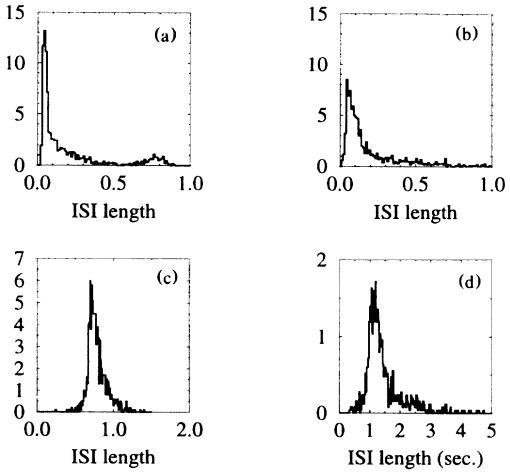

FIG. 6. Sample probability density functions (histograms) of ISI series. (a) Deterministic series from Fig. 5(a). (b) Stochastic series from Fig. 5(b). (c) Deterministic series, from Lorenz with $S(t) = x^2$ and $\Theta = 50$. (d) Series recorded from experiment.

diction algorithm applied to the stochastically driven ISI series. The deterministic structure present in Fig. 5(a) has been clearly destroyed in 5(b). Figures 6(a) and 6(b) compare the histograms of ISI's of the deterministically and stochastically generated processes. Note in particular that the second peak of the bimodal histogram of the deterministically driven system is eliminated in the stochastic case.

A final question we raise for further investigation is to what extent the ISI's we have synthesized using generic chaotic attractors resemble ISI's from experimental data. Figure 6(c) shows sample probability distributions of ISI's for the Lorenz and integrate-and-fire model, with $S(t) = x^2$ and $\Theta = 50$. Figure 6(d) shows a probability distribution of ISI's from an experiment which recorded spontaneous firing in the CA3 region of an *in vitro* rat hippocampal slice in a high concentration potassium medium. The data from this experiment are analyzed in [20].

I am grateful to Steven Schiff and Andre Longtin for helpful discussions. This research was supported in part by the NSF (Computational Mathematics and Physics programs), and DOE (Office of Scientific Computing).

[1] N. Packard, J. Crutchfield, J.D. Farmer, and R. Shaw, Phys. Rev. Lett. **45**, 712 (1980).
[2] F. Takens, in *Dynamical Systems and Turbulence*, edited by D.A. Rand and L.-L. Young, Lecture Notes in Mathematics Vol. 898 (Springer-Verlag, Berlin, 1981).
[3] T. Sauer, J.A. Yorke, and M. Casdagli, J. Stat. Phys. **65**, 579 (1991).
[4] Reviews of nonlinear noise reduction techniques are available: P. Grassberger, R. Hegger, H. Kantz, C. Schaffrath, and T. Schreiber, Chaos **3**, 127 (1993). E.J. Kostelich and T. Schreiber, Phys. Rev. E **48**, 1752 (1993).
[5] J.D. Farmer and J.J. Sidorowich, Phys. Rev. Lett. **59**, 845 (1987).
[6] *Time Series Prediction: Forecasting the Future and Understanding the Past*, edited by A.S. Weigend and N.A. Gershenfeld, Santa Fe Institute Studies in the Science of Complexity XV (Addison-Wesley, Reading, MA, 1993).
[7] T. Shinbrot, C. Grebogi, E. Ott, and J.A. Yorke, Nature (London) **363**, 411 (1993).
[8] *Stochastic Point Processes: Statistical Analysis, Theory, and Applications*, edited by P.A.W. Lewis (Wiley-Interscience, New York, 1972).
[9] H. Preissl, A. Aertsen, and G. Palm, in *Parallel Processing in Neural Systems and Computers*, edited by R. Eckmiller, G. Hartmann, and G. Hauske (Elsevier, Amsterdam, 1990), p. 83.
[10] A. Longtin, Int. J. Bif. Chaos **3** (1993). A. Longtin, A. Bulsara, and F. Moss, Phys. Rev. Lett. **67**, 656 (1991).
[11] H. Tuckwell, *Introduction to Theoretical Neurobiology* (Cambridge University Press, Cambridge, 1988), Vols. 1 and 2.
[12] E. Lorenz, J. Atmos. Sci. **20**, 130–141 (1963).
[13] T. Sauer (to be published).
[14] O. Rössler, Z. Naturforsch. **31**, 1168–1172 (1976).
[15] G. Sugihara and R.M. May, Nature (London) **344**, 734 (1990).
[16] J. Theiler, S. Eubank, A. Longtin, B. Galdrakian, and J.D. Farmer, Physica (Amsterdam) **58D**, 77 (1992).
[17] D.T. Kaplan and L. Glass, Phys. Rev. Lett. **68**, 427 (1992).
[18] R. Wayland, D. Bromley, D. Pickett, and A. Passamante, Phys. Rev. Lett. **70**, 580 (1993).
[19] P. Grassberger and I. Procaccia, Phys. Rev. Lett. **50**, 346 (1983).
[20] S.J. Schiff, K. Jerger, T. Chang, T. Sauer, and P.G. Aitken (to be published).

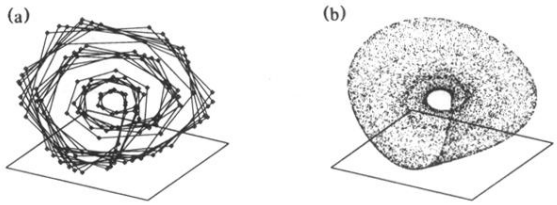

FIG. 2. Reconstructed phase portrait for the Rössler attractor using ISI's. (a) 150 ISI's connected by line segments. (b) 10 000 ISI's shown.